

VERY COLD AND MASSIVE CORES NEAR ISOSS J18364-0221: IMPLICATIONS FOR THE INITIAL CONDITIONS OF HIGH-MASS STAR-FORMATION

STEPHAN M. BIRKMANN¹, OLIVER KRAUSE^{1,2}, AND DIETRICH LEMKE¹

Accepted for publication in the Astrophysical Journal

ABSTRACT

We report the discovery of two very cold and massive molecular cloud cores in the region ISOSS J18364-0221. The object has been identified by a systematic search for very early evolutionary stages of high-mass stars using the 170 μm ISOPHOT Serendipity Survey (ISOSS). Submm continuum and molecular line measurements reveal two compact cores within this region. The first core has a temperature of 16.5 K, shows signs of ongoing infall and outflows, has no NIR or MIR counterpart and is massive enough ($M \sim 75 M_{\odot}$) to form at least one O star with an associated cluster. It is therefore considered a candidate for a genuine high-mass protostar and a high-mass analog to the Class 0 objects. The second core has an average gas and dust temperature of only ~ 12 K and a mass of $M \sim 280 M_{\odot}$. Its temperature and level of turbulence are below the values found for massive cores so far and are suggested to represent the initial conditions from which high-mass star formation occurs.

Subject headings: Stars: formation — ISM: dust, extinction — ISM: kinematics and dynamics — ISM: clouds — ISM: individual objects: ISOSS J18364-0221 — Astronomical data bases: ISO data base

1. INTRODUCTION

Most of the current knowledge about the formation and early evolution of high-mass stars has been inferred from observations of luminous infrared sources: High-mass protostellar objects (HMPO) (Sridharan et al. 2002) and hot molecular cores (HMCs) (Kurtz et al. 2000), both among the youngest known manifestations of high-mass stars, are dense condensations of warm ($T > 30$ K) gas and dust. Given their high luminosity of $L_{\text{IR}} > 10^3 L_{\odot}$ most of these objects were readily detected by the IRAS mission and have been identified by using color criteria on their infrared fluxes (e.g. Fontani et al. 2005; Williams et al. 2004; Molinari et al. 2002; Henning et al. 2000a).

Much less is known about a potential evolutionary stage prior to the HMPO/HMC phase. It has been suggested that very cold ($T \sim 10$ K) and massive cores might represent the initial conditions from which massive stars form (Evans et al. 2002), similar to the pre-stellar cores in the low-mass regime (Ward-Thompson 2002). Although promising candidates for very young protostars have been recently discovered near more evolved and luminous objects (Garay et al. 2004; Forbrich et al. 2004; Wu et al. 2005), no clear example of such a very cold core is known so far.

Using the 170 μm ISOPHOT Serendipity Survey (ISOSS) (Lemke et al. 1996; Bogun et al. 1996) we have performed an unbiased search for such very cold sources based on their $F_{170\mu\text{m}}/F_{100\mu\text{m}}$ color. By cross-correlating the ISOSS catalog with the IRAS point source catalog and molecular line surveys, we have identified more than 50 massive ($M > 100 M_{\odot}$) candidate sources with a flux ratio of $F_{170\mu\text{m}}/F_{100\mu\text{m}} > 2$, implying average dust tem-

peratures lower than 18 K (Krause et al. 2004).

We have launched multi-wavelength follow-up observations to explore the physical conditions in this unique sample of cold and massive star forming regions (e.g. Krause et al. 2003). In this letter we report the discovery of extremely cold and massive cloud cores in the region ISOSS J18364-0221 which provide new constraints on the physical conditions under which high-mass stars form.

2. OBSERVATIONS

Fig. 1 shows far-infrared observations of ISOSS J18364-0221. The object was centrally crossed by two detector pixels of the C200 camera onboard ISO (beam size of 1.5' *FWHM*) during an ISOSS scan. A 170 μm flux $F_{170\mu\text{m}} = 235 \pm 47$ Jy has been derived using procedures by Krause (2003) and Stickel et al. (2004). The compact ISOSS source coincides in position with the unresolved IRAS point source 18339-0224 (R.A. (2000)=18^h36^m24^s.7, DEC. (2000)=−02°21'49") which has previously been detected in the CO(1-0) transition (Yang et al. 2002). Its CO radial velocity of $v_{\text{LSR}} \sim 33$ km/s corresponds to a kinematical distance of $d \sim 2.2$ kpc according to Brand & Blitz (1993). This is consistent with the distance derived by the empirical relation $d = 320N^{0.57}$ pc, where N is the number of foreground stars detected on the POSS-B image inside a 5' aperture towards the cloud (Herbst & Sawyer 1981).

Submm continuum jiggle maps at 850 μm and 450 μm were obtained with SCUBA (Holland et al. 1999) at the James Clerk Maxwell Telescope (JCMT) in May 2003 under good atmospheric transmission conditions ($\tau_{225\text{GHz}} = 0.067 \pm 0.003$). The data was reduced with SURF, including sky noise reduction, yielding a photometric accuracy of 20% (450 μm) and 12% (850 μm). The beam size is 7.5" and 14.5", respectively.

Observations of the Ammonia inversion lines (J,K) = (1,1), (2,2), (3,3), and (4,4) were carried out at the Effelsberg 100 m telescope in January 2003. The beam size at

Electronic address: birkmann@mpia.de
Electronic address: krause@as.arizona.edu
Electronic address: lemke@mpia.de

¹ Max-Planck-Institut für Astronomie, Königstuhl 17, D-69117 Heidelberg, Germany

² Steward Observatory, University of Arizona, Tucson, AZ 85721

the observing frequency of 23.7 GHz is $40''$. The pointing accuracy is estimated to $5''$ rms and the flux uncertainty to 10%.

Molecular line measurements of CO(2-1) and C¹⁸O(2-1) (beam size $\sim 11''$), HCO⁺(3-2) and H¹³CO⁺(3-2) (beam size $\sim 9.5''$) were obtained at the IRAM 30 m in November 2003 and of CO(3-2) (beam size $\sim 22''$) at the Heinrich Hertz Telescope in December 2004. We used the facility receivers and reduced all spectra with the CLASS software. The atmospheric transmission was ($\tau_{225\text{GHz}} \sim 0.15$) for the HCO⁺(3-2) ($\tau_{225\text{GHz}} \sim 0.5$) for the CO(2-1) and ($\tau_{225\text{GHz}} \sim 0.1$) for the CO(3-2) observations. The estimated pointing error for both telescopes is $3''$ and the radiometric accuracy 15%.

Near infrared images in J, H, and Ks have been obtained at the Calar Alto 3.5 m telescope in Oktober 2003 and June 2004 with Omega2000 and OmegaPrime. Data reduction was carried out using standard procedures in IRAF. Photometric calibration is based on the 2MASS point source catalog.

3. RESULTS

Fig. 2 displays contours of SCUBA $850\ \mu\text{m}$ emission towards ISOSS J18364-0221 overlaid onto a near-infrared color composite. The IRAS and ISOSS FIR point source is clearly resolved into two emission peaks in the submillimeter. The *FWHM* is $17'' \times 10.5''$ (PA $\sim -10^\circ$) for the eastern core (SMM1), while the western core (SMM2) is more extended. The fluxes are $F_{850\ \mu\text{m}} = 2.11\ \text{Jy}$ and $F_{450\ \mu\text{m}} = 13.5\ \text{Jy}$ for SMM1 and $F_{850\ \mu\text{m}} = 2.85\ \text{Jy}$ and $F_{450\ \mu\text{m}} = 15.8\ \text{Jy}$ for SMM2. In addition to the photometric uncertainties of the submm fluxes, the $850\ \mu\text{m}$ flux may be contaminated by the CO(3-2) transition. We checked the CO(3-2) contribution in the SCUBA $850\ \mu\text{m}$ band using our HHT CO(3-2) map and found the level to be within our overall calibrational uncertainty. Derivation of the dust temperature from submm data alone heavily depends on the chosen dust emissivity index β for which values between 1 and 2 are reported in the literature. Using an emissivity index of $\beta = 2$ we find $T_d = 14\ \text{K}$ for SMM1 and $T_d = 12\ \text{K}$ for SMM2. For lower values of β the temperatures would be higher. In order to constrain both β and the dust temperature we use the measured $100\ \mu\text{m}$ flux ($F_{100\ \mu\text{m}} = 57.7\ \text{Jy}$) of the whole ISOSS J18364-0221 cloud that places an upper limit for the emission of the individual cores. Using HIRES processed maps of the region, we find that the relative flux ratio of SMM1 to SMM2 at $100\ \mu\text{m}$ is approximately 10:1. Using this ratio we derive $\beta = 1.6$ and $T_d = 21\ \text{K}$ for SMM1 and $\beta = 1.8$ and $T_d = 13.8\ \text{K}$ for SMM2. Since this is an upper limit we take the average values for the rest of the paper: $\beta = 1.8 \pm 0.2$, $T_d = 16.5_{-3}^{+6}\ \text{K}$ and $\beta = 1.9 \pm 0.1$, $T_d = 12.8_{-1.5}^{+2.0}\ \text{K}$ for SMM1 and SMM2, respectively.

We estimate the masses of the cores using the relation of Hildebrand (1983) $M_d = F_\lambda d^2 / \kappa_\lambda B_\lambda(T)$ with a gas-to-dust ratio of 100. The mass of SMM1 is $M = 75 \pm 30\ M_\odot$, SMM2 has a mass of $M = 280_{-60}^{+75}\ M_\odot$. We used $\kappa_{850\ \mu\text{m}} = 0.018$ for SMM1 (gas+dust, thin icemantles, $n \sim 10^6\ \text{cm}^{-3}$) and for SMM2 $\kappa_{850\ \mu\text{m}} = 0.010$ (gas+dust, thin icemantles) taking the values from Ossenkopf & Henning (1994)).

The submillimeter emission is highly correlated with

the NIR extinction, as seen by the reddening and surface density of background stars in Fig. 2. We have constructed a quantitative extinction map from our J, H, and Ks images according to the NICER method of Lombardi & Alves (2001) (Fig. 3). The map reveals that the compact far-infrared and submm sources are embedded in the center of a much more extended cloud complex which is also visible as an optical dark cloud Lynds 541.

In contrast to the submillimeter maps which resolve individual features on typical scales of individual cloud cores (0.1 pc), the ISOSS and IRAS beams constrain the average temperature and mass of the whole dense cloud center on approximately 1 pc scale. The small chopping throw of SCUBA ($2''$) results in spatial filtering of structures that are comparable or larger in size. We account for an average column density of $A_V \sim 7$ (see Fig. 3) to correct the integrated flux of the chopped SCUBA measurements. We fit a single modified black body to the data longwards of $100\ \mu\text{m}$ (Fig. 4) and derive a temperature of $14.6_{-1.0}^{+1.2}\ \text{K}$ and $\beta = 2$. The total luminosity of ISOSS J18364-0221 is $L \sim 800\ L_\odot$.

The mass of the region is $M = 900_{-330}^{+450}\ M_\odot$ ($\kappa_{170\ \mu\text{m}} = 25\ \text{cm}^2\ \text{g}^{-1}$) with the uncertainty dominated by the derived average dust temperature. A lower limit for the mass can be computed from our extinction map, using the relation $M = (\Delta\Omega d)^2 \mu \frac{N_H}{A_V} \sum_i A_V(i)$ given by Dickman (1978). With a dust-to-gas ratio of $N_H/A_V = 1.87 \times 10^{21}\ \text{cm}^{-2}\ \text{mag}^{-1}$ (Savage & Mathis 1979) we obtain a mass of $M \geq 460\ M_\odot$ for ISOSS J18364-0221 and $M \sim 3200\ M_\odot$ for the whole complex shown in Fig. 3.

Ammonia (NH₃) is an ideal temperature probe for the molecular gas in dense regions (Harju et al. 1993; Walmsley & Ungerechts 1983). From the relative intensity of the (J,K) = (1,1) and (2,2) inversion transitions of our ammonia (NH₃) data, we derive a gas kinetic temperature of $T_{\text{kin}} = 11.6 \pm 1.5\ \text{K}$ towards SMM2 (Fig. 5). The inversion transitions (J,K) = (3,3) and (4,4) were not detected in neither of the cores ($\sigma_{\text{RMS}} \sim 30\ \text{mK}$). The latter transitions have been used as sensitive tracers of HMCs and argue against the presence of such an object in ISOSS J18364-0221. SMM2 has a shallow density profile and is larger than the beam size of the ammonia measurements ($40''$). Therefore beam dilution is neglectable and we can directly compare the line and continuum measurements. The good match of T_{kin} and T_d (in particular for $\beta = 2$) suggests thermal coupling between dust and gas, as it is expected for cold and dense cores.

4. DISCUSSION

We now discuss the nature of the two massive cold cores in ISOSS J18364-0221 and the implications for the initial conditions of high-mass star formation.

SMM1 is cold ($T \approx 16.5\ \text{K}$) and compact (effective radius $R \sim 0.2\ \text{pc}$). From our $450\ \mu\text{m}$ data we derive a column density of $N(\text{H}_2) = 2.2 \times 10^{23}\ \text{cm}^{-2}$ and a minimum central density of $n(\text{H}_2) = 1.4 \times 10^6\ \text{cm}^{-3}$. Our measurement of optically thin H¹³CO⁺(3-2) transition towards SMM1 (Fig. 6) provides an independent check for the temperature and (column) density of the high-density gas. Using the density and temperature from the dust continuum and applying the radiative transfer code from Schöier et al. (2005), we find an abundance of [HCO/H₂] of 8×10^{-10} which is in good agreement with the value

predicted for protostellar cores (Bergin & Langer 1997). Our molecular line measurements further indicate that the core is collapsing and drives an outflow: The optically thick $\text{H}^{12}\text{CO}^+(3-2)$ transition shows a red-shifted self absorption with respect to the optically thin $\text{H}^{13}\text{CO}^+(3-2)$ line (Fig. 6), suggesting large scale infall towards the center of the core (Choi 2002; Evans 1999). The CO(2-1) spectra show significant line wings around the two submm cores when compared with $\text{C}^{18}\text{O}(2-1)$, indicating the presence outflows (see Fig. 2). We derived the outflow parameters using our CO(2-1) and $\text{C}^{18}\text{O}(2-1)$ data following Henning et al. (2000b). The mass of the outflow is estimated to $M_f \approx 18 M_\odot$ and the dynamical timescale t_d is $\sim 1.8 \times 10^4$ years. The corresponding mass outflow rate is $\dot{M} \approx 1 \times 10^{-3} M_\odot/\text{yr}$ and the momentum supply rate $F \approx 8.5 \times 10^{-3} M_\odot \text{ km s}^{-1}/\text{yr}$, without correcting for the unknown inclination i of the outflow. This correction would further increase the derived values, which are already comparable to those observed for outflows in high-mass star forming regions (e.g. Beuther et al. 2002; Zhang et al. 2005). It must be noted however that both the red and blue lobes have complex morphologies and higher resolution observations are required to decide on the actual number of outflows driven by SMM1. No infrared counterpart is detected in our deep near-infrared images nor in the MSX mid-infrared data, which is however not surprising considering the extinction of $A_V \geq 120$. With $M \sim 75 M_\odot$ SMM1 would be massive enough to form an O type star and an associated cluster. We therefore consider SMM1 as a promising candidate for a massive protostar during its initial gravitational collapse, i.e. in an evolutionary state comparable to the Class 0 phase in low-mass star formation.

SMM2 has very low gas and dust temperatures ($T \approx 12 \text{ K}$), moderate densities (central density $n(\text{H}_2) \sim 2.3 \times 10^5 \text{ cm}^{-3}$), and is quite extended (effective radius $R \sim 0.5 \text{ pc}$). Such conditions have been suggested to characterize the earliest stage of star formation (Evans et al. 2002), but have so far only been observed in low-mass prestellar cores. We investigate the dynamical state of the core considering the virial theorem, with $E_{\text{mag}} + E_{\text{pot}} = 2(E_{\text{kin}} - E_{\text{ext}})$ being the condition for a gravitationally bound core. E_{mag} denotes the magnetic energy, E_{pot} is the potential energy, E_{kin} the total kinetic energy, and E_{ext} accounts

for external pressure. The kinetic energy can be written as $E_{\text{kin}} = E_{\text{therm}} + E_{\text{turb}} = \frac{3}{2}NkT + \frac{3}{2}M\sigma_{\text{turb}}^2$, with $\sigma^2 = \Delta V^2/(8 \ln 2) - kT/m$, where $\Delta V = 0.90 \text{ km/s}$ is the linewidth taken from our ammonia data (Fig. 5) and m the mass of the NH_3 molecule. The potential energy of a homogenous ellipsoid is $E_{\text{pot}} = 3GM^2/5R$ (Liljestrom 1991). We find $E_{\text{pot}} = 9.5 \times 10^{38} \text{ J}$, $E_{\text{therm}} = 3.1 \times 10^{37} \text{ J}$, and $E_{\text{turb}} = 1.2 \times 10^{38} \text{ J}$. Neglecting the external pressure and the magnetic field energy the total kinetic energy sums up to $\sim 16\%$ of the potential energy. We conclude that SMM2 is Jeans unstable. The small line width of the optically thin ammonia transitions suggests that the level of turbulence is not as high as in more evolved high-mass cores. There are two sources with very red colors towards SMM2 (H-K=3.7 and H-K=4.5) that are presumably low-mass Class I objects, based on their NIR and MIR fluxes with a spectral index of $a = d \log(\lambda F_\lambda)/d \log(\lambda) \sim 3$. This classification is supported by the molecular outflow traced in CO(2-1) emerging from the young stellar objects (Fig. 2). This supports the large-scale Jeans instability of the core and indicates that fragmentation and cluster formation has already started. Therefore SMM2 is a very promising candidate for a massive pre-stellar core, characterizing the earliest phase of star formation.

Several authors (e.g. Evans et al. 2002) have suggested that the conditions during the earliest phases of high-mass star-formation should be similar to that prevailing in the regime of low-mass star birth. Our findings provide direct observational evidence that the initial conditions of high-mass star-formation are indeed characterized by very low temperatures and low levels of turbulence.

We like to thank the anonymous referee for the helpful comments and suggestions that improved our paper significantly. We acknowledge the support of L.V. Tóth and H. Beuther in the ammonia measurements. Based on observations with the Infrared Space Observatory, the Calar Alto 3.5 m telescope, the IRAM 30 m, the Effelsberg 100-m telescope of the Max-Planck-Institut für Radioastronomie, the James-Clerk-Maxwell Telescope and the Heinrich-Hertz-Telescope. The ISOSS is supported by funds from the DLR, Bonn.

REFERENCES

- Bergin, E. A., & Langer, W. D. 1997, *ApJ*, 486, 316
 Beuther, H., Schilke, P., Sridharan, T. K., Menten, K. M., Walmsley, C. M., & Wyrowski, F. 2002, *A&A*, 383, 892
 Bogun, S., et al. 1996, *A&A*, 315, L71
 Brand, J., & Blitz, L. 1993, *A&A*, 275, 67
 Choi, M. 2002, *ApJ*, 575, 900
 Dickman, R. L. 1978, *AJ*, 83, 363
 Evans, N. J. 1999, *ARA&A*, 37, 311
 Evans, N. J., Shirley, Y. L., Mueller, K. E., & Knez, C. 2002, *ASP Conf. Ser.* 267: Hot Star Workshop III: The Earliest Phases of Massive Star Birth, 267, 17
 Fontani, F., Beltrán, M. T., Brand, J., Cesaroni, R., Testi, L., Molinari, S., & Walmsley, C. M. 2005, *A&A*, 432, 921
 Forbrich, J., Schreyer, K., Posselt, B., Klein, R., & Henning, T. 2004, *ApJ*, 602, 843
 Garay, G., Faúndez, S., Mardones, D., Bronfman, L., Chini, R., & Nyman, L. 2004, *ApJ*, 610, 313
 Harju, J., Walmsley, C. M., & Wouterloot, J. G. A. 1993, *A&AS*, 98, 51
 Henning, T., Schreyer, K., Launhardt, R., & Burkert, A. 2000, *A&A*, 353, 211
 Henning, T., Lapinov, A., Schreyer, K., Stecklum, B., & Zinchenko, I. 2000, *A&A*, 364, 613
 Herbst, W., & Sawyer, D. L. 1981, *ApJ*, 243, 935
 Hildebrand, R. H. 1983, *QJRAS*, 24, 267
 Holland, W. S., et al. 1999, *MNRAS*, 303, 659
 Krause, O. 2003, Ph.D. Thesis, University of Heidelberg
 Krause, O., Lemke, D., Tóth, L. V., Klaas, U., Haas, M., Stichel, M., & Vavrek, R. 2003, *A&A*, 398, 1007
 Krause, O., Vavrek, R., Birkmann, S., Klaas, U., Stichel, M., Tóth, L. V., & Lemke, D. 2004, *Baltic Astronomy*, 13, 407
 Kurtz, S., Cesaroni, R., Churchwell, E., Hofner, P., & Walmsley, C. M. 2000, *Protostars and Planets IV*, 299
 Lemke, D., et al. 1996, *A&A*, 315, L64
 Liljestrom, T. 1991, *A&A*, 244, 483
 Lombardi, M., & Alves, J. 2001, *A&A*, 377, 1023
 Molinari, S., Testi, L., Rodríguez, L. F., & Zhang, Q. 2002, *ApJ*, 570, 758
 Ossenkopf, V., & Henning, T. 1994, *A&A*, 291, 943
 Robin, A. C., Reylé, C., Derrière, S., & Picaud, S. 2003, *A&A*, 409, 523
 Savage, B. D., & Mathis, J. S. 1979, *ARA&A*, 17, 73
 Schöier, F. L., van der Tak, F. F. S., van Dishoeck, E. F., & Black, J. H. 2005, *A&A*, 432, 369
 Sridharan, T. K., Beuther, H., Schilke, P., Menten, K. M., & Wyrowski, F. 2002, *ApJ*, 566, 931

- Stickel, M., Lemke, D., Klaas, U., Krause, O., & Egner, S. 2004, A&A, 422, 39
- Walmsley, C. M., & Ungerechts, H. 1983, A&A, 122, 164
- Ward-Thompson, D. 2002, Science, 295, 76
- Williams, S. J., Fuller, G. A., & Sridharan, T. K. 2004, A&A, 417, 115
- Wu, Y., Zhu, M., Wei, Y., Xu, D., Zhang, Q., & Fiege, J. D. 2005, ApJ, 628, L57
- Yang, J., Jiang, Z., Wang, M., Ju, B., & Wang, H. 2002, ApJS, 141, 157
- Zhang, Q., Hunter, T. R., Brand, J., Sridharan, T. K., Cesaroni, R., Molinari, S., Wang, J., & Kramer, M. 2005, ApJ, 625, 864

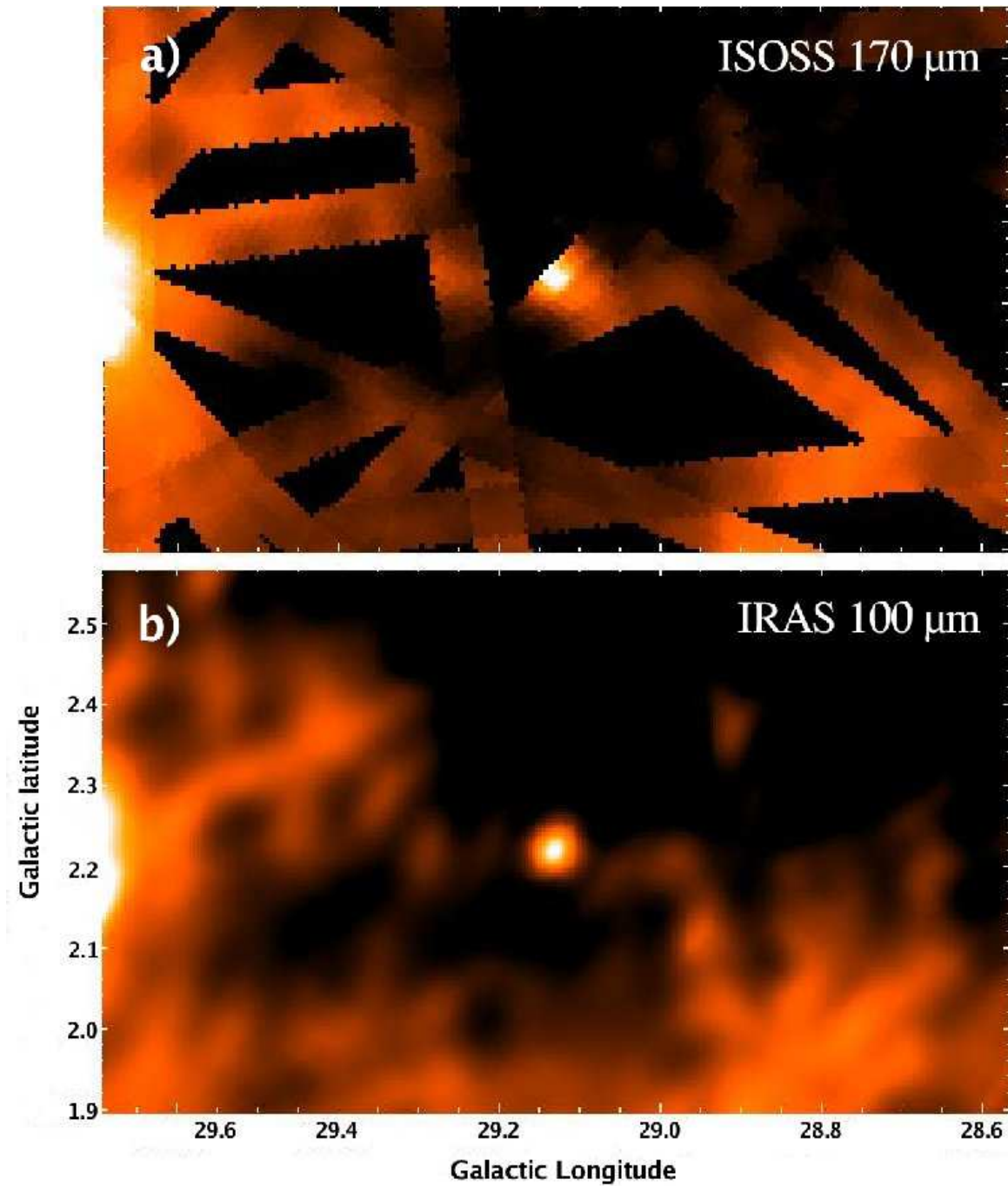


FIG. 1.— a) Incomplete 170 μm map constructed from slew-measurement by the ISOPHOT Serendipity Survey. ISOSS J18364-0221 is the compact source in the center. b) 100 μm map of the same field, produced by HIRES processing of the IRAS survey.

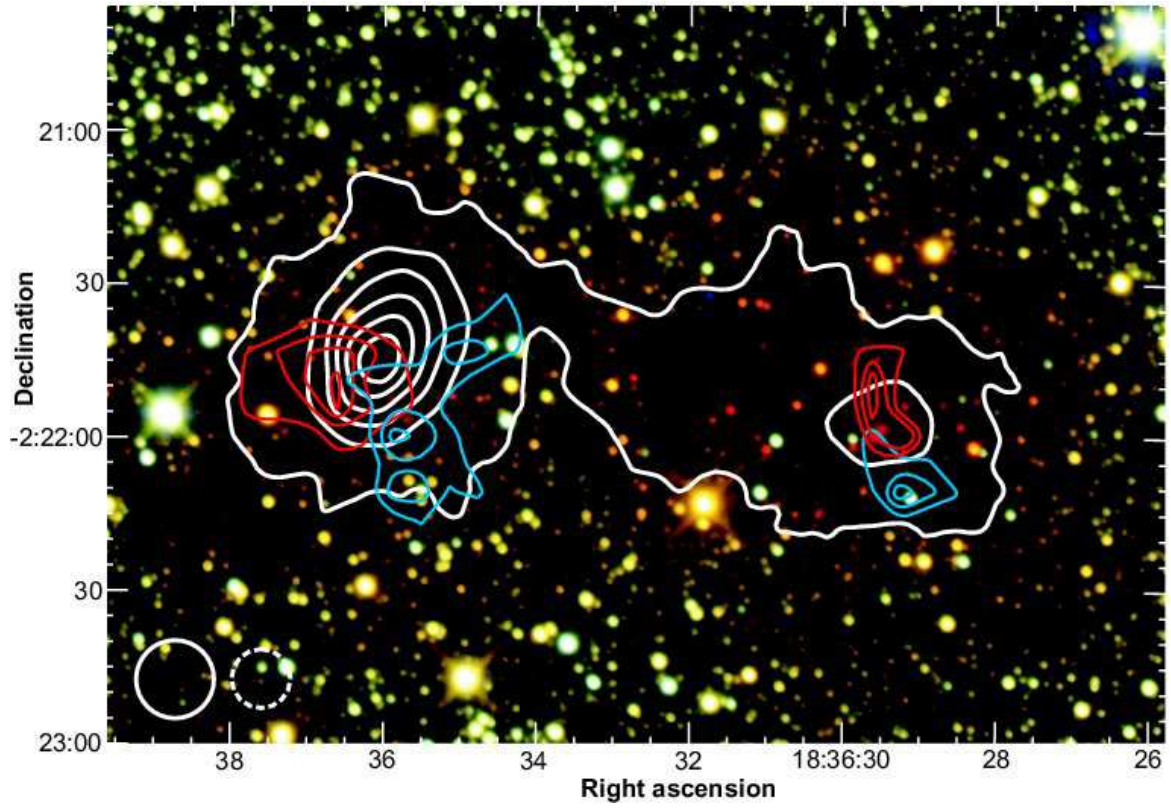


FIG. 2.— ISOSS J18364-0221 in JHKs, the white contours give the 850 μ m flux at levels of 50, 150, 250, +200 mJy/beam. The thin contours show the red ($v[40 - 52]$ km s⁻¹) and blue ($v[22 - 30]$ km s⁻¹) CO(2-1) emission. The beam sizes are denoted in the lower left.

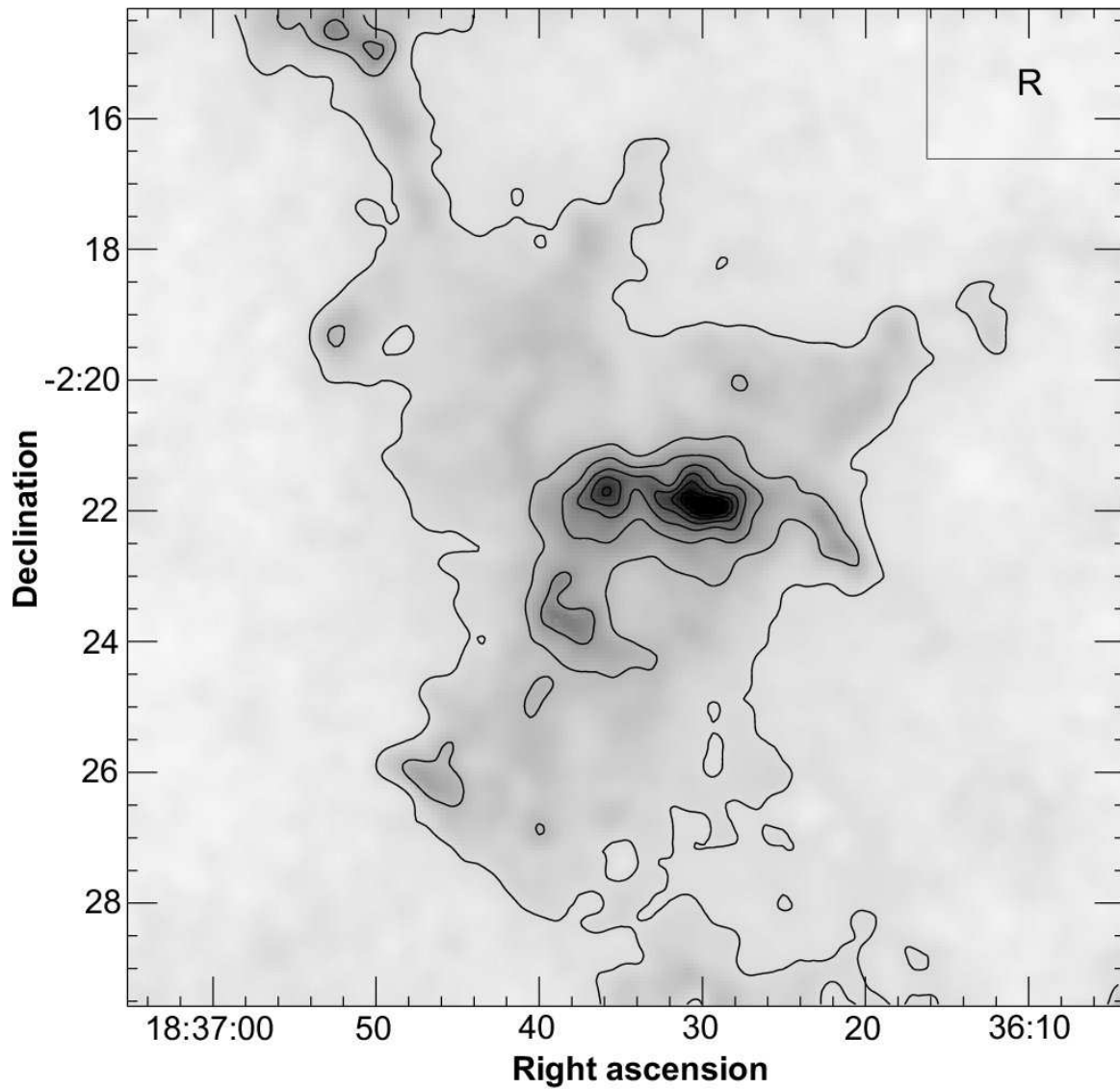


FIG. 3.— Map of the visual extinction A_V towards ISOSS J18364-0221. Contours start at $A_V = 4$ and increase in steps of 4. The local extinction was determined from the reference region R. Colors for zero extinction were established using a simulated besancon model catalog (Robin et al. 2003) towards the region.

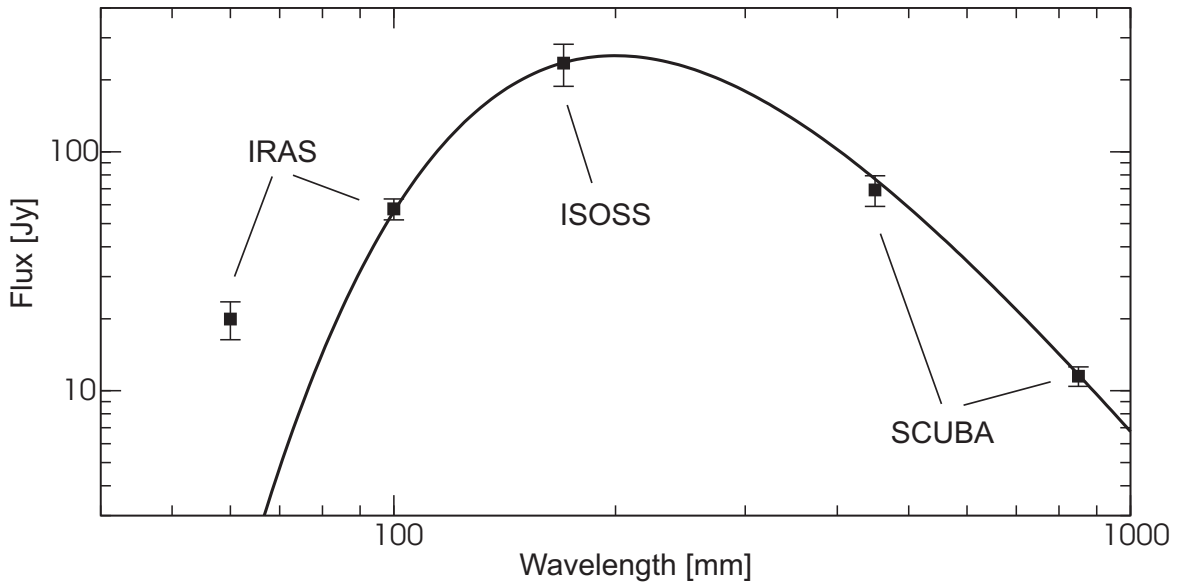


FIG. 4.— Spectral energy distribution of ISOSS J18364-0221. For wavelengths longwards of $100 \mu\text{m}$ the SED is dominated by the optically thin thermal emission of large grains and well fitted with a modified black body with an emissivity index of $\beta = 2$, the point at $60 \mu\text{m}$ is not taken into account.

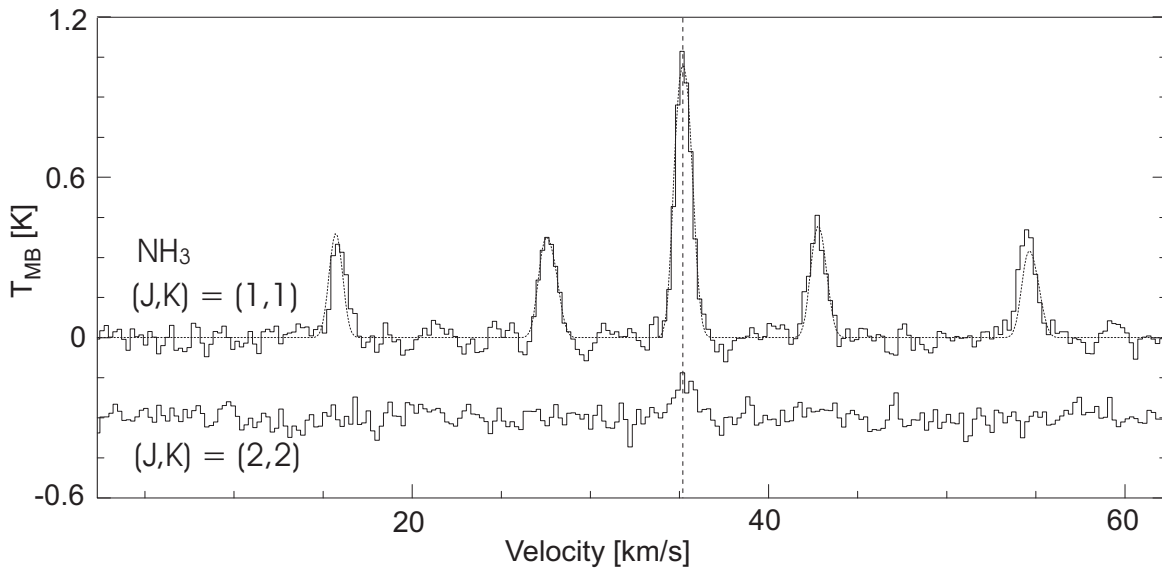


FIG. 5.— Spectra of the NH_3 $(J,K) = (1,1)$ and $(2,2)$ inversion transitions towards ISOSS J18339-0221 SMM2. A fit to the hyperfine structure of the $(1,1)$ line is also shown.

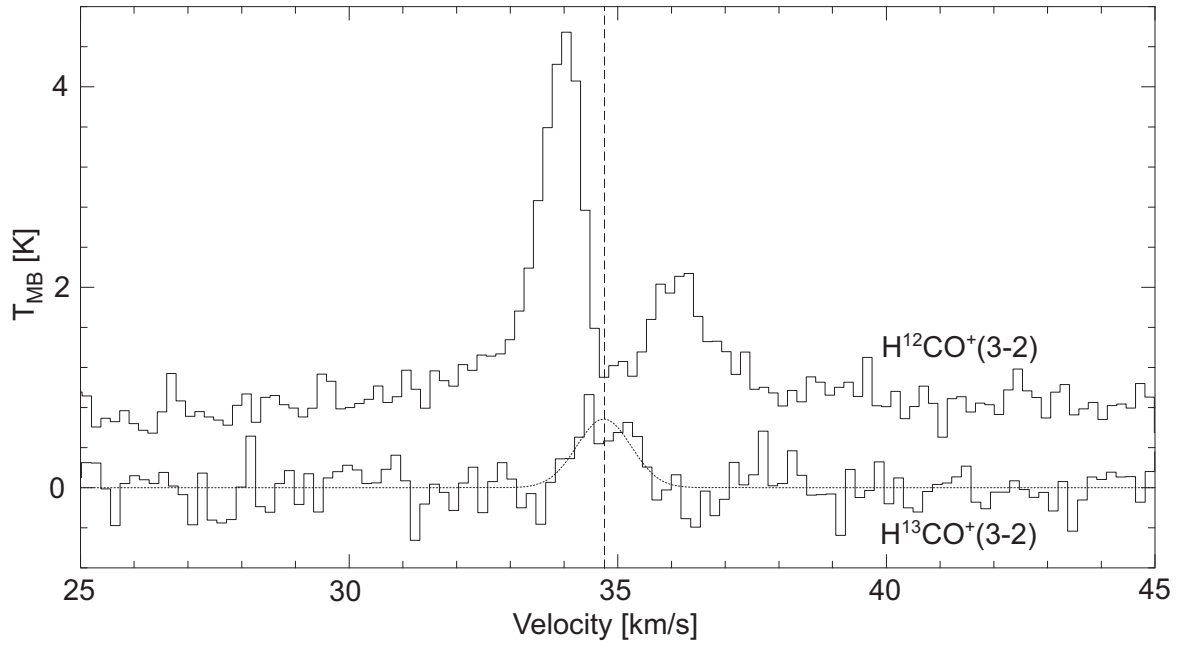


FIG. 6.— $\text{H}^{12}\text{CO}^+(3-2)$ and $\text{H}^{13}\text{CO}^+(3-2)$ taken at SMM1. The vertical dashed line marks the central velocity of the optical thin line, the optically thick transition shows red-shifted self absorption.